ELSEVIER

Catalysis Today 28 (1996) 335–350

CATALYSIS TODAY

The dynamic states of silica-supported metal oxide catalysts during methanol oxidation

Jih-Mirn Jehng [b], Hungchun Hu [a], Xingtao Gao [a], Israel E. Wachs [a,*]

[a] *Zettlemoyer Center for Surface Studies, Department of Chemical Engineering, Lehigh University, Bethlehem, PA 18015, USA*
[b] *Department of Chemical Engineering, National Chung-Hsing University, 250, Kuokuang Road, Taichung 402, Taiwan, ROC*

Abstract

The in situ Raman spectra of silica-supported metal oxide catalysts (containing surface metal oxide species of V, Nb, Cr, Mo, W and Re) were measured during methanol oxidation. Stable surface methoxy species were found to form via reaction with the surface Si-OH groups for all the catalysts investigated. The surface Si-OH groups were also titrated by the surface metal oxide species and the surface concentration of Si-OH groups decreases with increasing metal oxide loading. The stable surface M-OCH_3 were only found for the V_2O_5/SiO_2 catalysts. The surface metal oxide species were all influenced by the methanol oxidation reaction. The surface rhenium oxide species were removed from the silica surface and the surface molybdenum oxide species were partially agglomerated to crystalline β-MoO_3 particles by the formation of Re-methoxy and Mo-methoxy complexes. The surface niobium oxide and tungsten oxide species were partially reducing by the net reducing methanol oxidation environment. In situ Raman spectra for the CrO_3/SiO_2 catalysts could not be obtained due to the formation of reduced chromium oxide species during methanol oxidation which gave rise to sample fluorescence. The in situ Raman observations provided a fundamental basis for understanding the selectivity patterns of the silica-supported metal oxide catalysts during methanol oxidation. However, the mechanism by which the silica support ligands activate the redox properties of the surface metal oxide species is not completely understood.

Keywords: Dynamic states; Silica-supported metal oxide catalysts; Methanol oxidation; Metal oxide catalysts

1. Introduction

Silica-supported metal oxide catalysts have been widely used in a number of reactions such as ethylene polymerization (CrO_3/SiO_2) [1–3], alkane oxidative dehydrogenation (V_2O_5/SiO_2) [4–8], the selective catalytic reduction of NO_x with ammonia [9] and the selective oxidation of methane (MoO_3/SiO_2) [10,11] and olefin metathesis (Re/SiO_2 and WO_3/SiO_2) [12]. These catalytic applications have generated much interested in the molecular structures of these catalysts and their relationship to the catalytic properties [13–29]. Furthermore, it is also of interest to modify the structures of the surface metal oxide species in order to improve their catalytic properties for specific applications.

It has generally been found that essentially the same surface dehydrated metal oxide species are present independent of the nature of the oxide support for each supported metal oxide system (such as V, Re, Cr and Mo) [22,29–32].

* Corresponding author.

PII S0920-5861(96)00047-8

The relative concentrations of the dehydrated surface metal oxide species, isolated (Raman bands in the 980-1038 cm^{-1} region) and polymerized (Raman bands in the 880-950 cm^{-1} region), appear to vary somewhat with the specific oxide support and the surface metal oxide coverage. However, the silica-supported metal oxide catalysts, especially SiO_2-based catalysts formed via high temperature pyrolysis, under dehydrated conditions contain isolated surface metal oxide species [33–35] because high surface coverages of metal oxides can not be achieved on the silica support due to the low number of the surface hydroxyl groups and their low reactivity. The molecular structures of the dehydrated surface metal oxide species on the silica support have been extensively characterized under in situ conditions by Raman spectroscopy [17–22,27–35], infrared spectroscopy [31,32,36,37], solid state ^{51}V NMR spectroscopy [38], X-ray absorption near edge spectroscopy (XANES) [30,39] and diffuse reflectance spectroscopy (DRS) [17,18,40]. These structural characterization studies revealed that the surface vanadium oxide species is present as a tetrahedral VO_4 structure with one terminal V = O bond (Raman band at 1037 cm^{-1}) and three V-O-Si bonds to the silica surface [38]. Four-fold coordinate surface NbO_4 species (Raman band at 980-990 cm^{-1}), with a structure similar to the surface vanadia species, is primarily found on the silica-supported niobia system [39]. An isolated surface molybdenum oxide species with a mono-oxo MoO structure has been reported for the silica-supported molybdenum oxide system [30] and the isolated surface rhenium oxide species with a tri-oxo ReO_4 structure have been suggested for the silica-supported rhenium oxide system [31]. An isolated tungsten oxide with a mono-oxo WO_5 has been proposed for the WO_3/SiO_2 system [41]. For the silica-supported chromium oxide system, the surface mono-chromate with a tetrahedral CrO_4 structure is predominantly present on the silica surface [17–19]. Thus, deposited metal oxides form incomplete surface metal oxide overlayers on the silica support and the molecular structures of the surface metal oxide species are dependent on the nature of the specific metal oxide. However, the molecular structures of these surface metal oxide species on silica during oxidation reactions are not known with the exception of the MoO_3/SiO_2 system [28].

The reactivity of the silica-supported metal oxide catalysts has been probed by the methanol oxidation reaction because it is very sensitive to the nature of the surface sites present in oxide catalysts [19,22,27,29]. Surface redox sites primarily form formaldehyde and methyl formate as the reaction products. Surface acid sites result in the formation of dimethyl ether. Methyl formate results from the combination of the CH_3O-group adsorbed on the silica surface and the H_2CO-group on the adjacent surface metal oxide sites [19]. Comparison of the reactivity of the different surface metal oxides on silica reveals that the TOF (turnover frequency) varies by two orders of magnitude [19,22]. The silica-supported chromium oxide has the highest TOF and the silica-supported vanadium oxide is the least active catalyst among these silica-supported metal oxide catalysts. Deo et al. performed catalytic studies on the surface vanadium oxide on different oxide supports and proposed that the reducibility of the V-O-Support bond is controlling the partial oxidation reactivity and that the oxide support appears to act as a ligand that influences the reactivity of surface metal oxide overlayer [22]. Thus, the reactivity of the silica-supported metal oxide is only dependent on the specific surface metal oxide species which is present on the silica surface. No systematic studies, however, have been performed to determine the behavior of the specific surface metal oxide species on SiO_2 during catalytic oxidation studies.

In this study, in situ Raman experiments during methanol oxidation reaction were performed over the silica-supported metal oxide catalysts in order to obtain insight into the fundamental factors affecting the reactivity and selectivity of these catalysts. Additional insights

into the structure-reactivity relationships of the silica-supported metal oxide catalysts were determined by relating the catalytic properties with the molecular structural information under reaction conditions.

2. Experimental

2.1. Materials and preparation

The silica-supported metal oxide catalysts were prepared by the incipient-wetness impregnation method. The SiO_2 (Cab-O-Sil, EH 5, ~ 380 m^2/g) support was pretreated with water and calcined at 500°C for 16 h under flowing dry air in order to condense its volume. The water pretreated procedure has no effect on the BET surface area of the silica support. For the air sensitive precursors, vanadium isopropoxide (Alfa, 95-99% purity) in a methanol solution (Fisher, 99.9% purity) and niobium ethoxide (Johnson Matthey, 99.999% purity) in a propanol solution were impregnated into the silica support under a nitrogen environment. The samples were initially dried at room temperature for 2 h to remove excess alcohol and further dried at 120°C for 16 h under flowing N_2. The samples were finally calcined at 500°C for 1 h under flowing N_2 and for an additional 15 h under flowing dry air to form the surface vanadium oxide species and surface niobium oxide on the SiO_2 support. A pentane solution of $W(\eta^3\text{-}C_3H_5)_4$ was used to prepare the silica-supported tungsten oxide catalyst by exchange reaction of C_3H_5 ligands with the silicas OH groups [41]. For the other precursors which are not air sensitive, chromium nitrate (Alfa, ACS), ammonium hepta-molybdate (Alfa, ACS) and perrhenic acid (Alfa, 99.9% purity) in aqueous solutions were used to impregnate the silica support. The samples were initially dried at 120°C for 16 h and further calcined at 500°C for 16 h under flowing dry air to form the surface chromium oxide, surface molybdenum oxide and surface rhenium oxide species on the silica support. Prior to Raman experiments, the silica-supported metal oxide catalysts were calcined at 600°C for 1 h under flowing dry air in order to removal the impurities which induce fluorescence on the silica surface.

2.2. Raman spectroscopy

2.2.1. In situ Raman spectroscopy

The in situ Raman spectrometer system consists of a quartz cell and a sample holder, a triple-grating spectrometer (Spex, Model 1877), a photodiode array detector (EG and G, Princeton Applied Research, Model 1420) and an argon ion laser (Spectra-Physics, Model 165). The sample holder is made from a metal alloy (Hastalloy C) and a 100-200 mg sample disc is held by the cap of the sample holder. The sample holder is mounted onto a ceramic shaft which is rotated by a 115 V DC motor at a speed of 1000-2000 rpm. A cylindrical heating coil surrounding the quartz cell is used to heat the sample and the temperature is measured by an internal thermocouple. The quartz cell is capable of operating up to 600°C and flowing gas is introduced into the cell at a rate of 100-300 cc/min at atmospheric pressure. The 514.5 nm line of the Ar^+ laser with 10-100 mW of power is focused on the sample disc in a right-angle scattering geometry. An ellipsoid mirror collects and reflects the scattered light into the spectrometers filter stage to reject the elastic scattering component. The resulting filtered light, consisting primarily of the Raman component of the scattered light, is collected with an EG and G intensified photodiode array detector which is coupled to the spectrometer and is thermoelectrically cooled to -35°C. The photodiode array detector is scanned with an EG and G OMA III optical multichannel analyzer (model 1463).

The in situ Raman spectra were obtained with the following procedure. The samples were placed into the cell and heated up to 500°C for 1 h in a flow of pure oxygen gas (Linde Specialty Grade, 99.99% purity). The dehydrated Raman

spectra were collected after cooling the sample to 230°C in a flow of pure oxygen gas for 30 min. After the above treatment, a gaseous mixture with a He/O_2 ratio near 11/6 containing saturated methanol vapor in the ice bath (~ 4 mol% CH_3OH) was introduced into the cell and the Raman spectra under reaction conditions were collected after reaching steady state (~ 30 min at the 230°C reaction temperature). Raman spectra were also recorded after the removal of methanol from the feed stream at 230°C. The catalysts were further reoxidized by flowing pure oxygen at 400°C for 1 h. Raman features of the surface metal oxide species appear in the 100-1200 cm^{-1} region and the surface methoxy species appear in the 2750-3100 cm^{-1} region.

3. Results

3.1. In situ raman spectra under methanol oxidation reaction

3.1.1. SiO_2

Previous in situ Raman studies on the silica support have shown that the dehydrated silica surface possesses Raman bands at ~ 1050 (the asymmetric mode of Si-O-Si linkages), ~ 979 (surface silanol groups), ~ 605 and ~ 488 (three- and four-fold siloxane rings), ~ 452 and 803 cm^{-1} (siloxane linkages) [42]. The in situ Raman spectra of the silica support during methanol oxidation are shown in Figs. 1 and 2. The weak Raman band at 2990 cm^{-1} is characteristic of the C-H asymmetric stretching vibration and the Raman bands at 2956 and 2856 cm^{-1} are characteristic of the C-H symmetric stretching vibrations of the surface methoxy groups on the silica support. These three bands are also detected by IR experiments and exhibit strong IR absorption signals [41]. Upon removal of methanol from the feed stream at 230°C, the surface methoxy groups are still present on the silica (see Fig. 1). Comparison of Raman features of the silica support under oxidizing conditions with those of the silica support under reaction conditions reveals a decrease in the Raman intensity of the Si-OH bond (970 cm^{-1}) during reaction as shown in Fig. 2. This indicates that the surface silanol groups partially

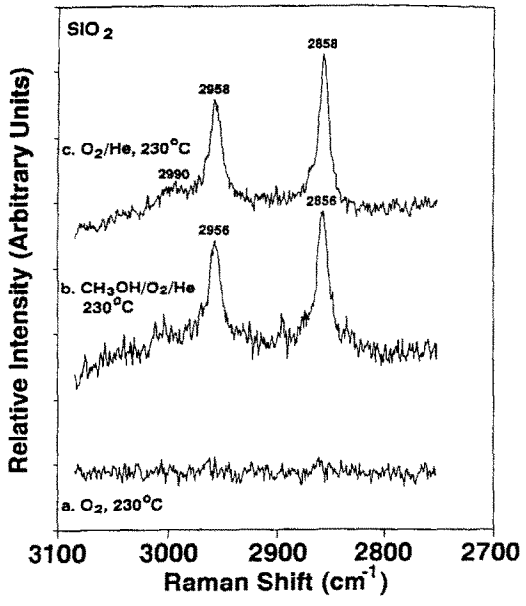

Fig. 1. In situ Raman spectra of the silica support at various stages of methanol oxidation reaction in the 2700–3100 cm^{-1} region.

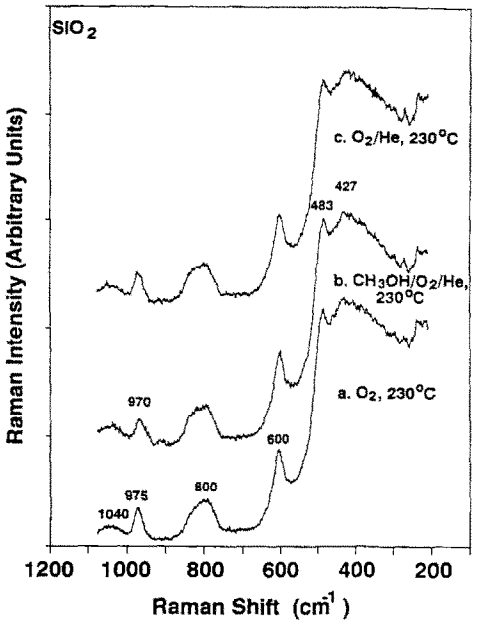

Fig. 2. In situ Raman spectra of the silica support upon methanol oxidation reaction in the 100–1200 cm^{-1} region.

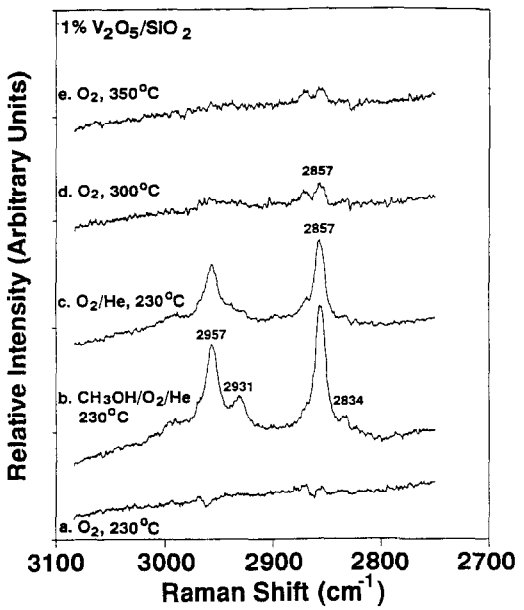

Fig. 3. In situ Raman spectra of the 1% V_2O_5/SiO_2 catalyst at various stages of methanol oxidation reaction in the 2700–3100 cm^{-1} region.

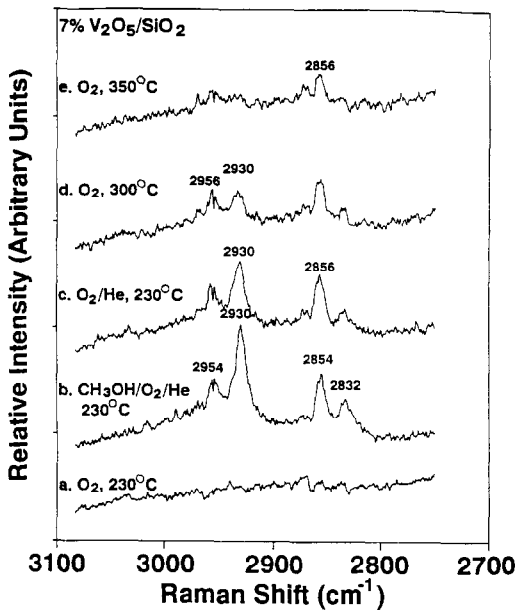

Fig. 4. In situ Raman spectra of the 7% V_2O_5/SiO_2 catalyst at various stages of methanol oxidation reaction in the 2700–3100 cm^{-1} region.

react with the methanol molecule to form a surface methoxy species.

3.1.2. V_2O_5/SiO_2

The in situ Raman spectra of the 1% and 7% V_2O_5/SiO_2 catalysts at various stages of reaction are shown in Figs. 3–6. During methanol oxidation, Raman bands at ~2990, ~2957, ~2931, ~2857 and ~2834 cm^{-1} appear and the intensity of the two Raman bands at 2931 and 2834 cm^{-1} increase with increasing surface vanadium oxide coverage (see Figs. 3 and 4). Prior to reaction, a sharp and strong Raman band is present at 1033-1035 cm^{-1} which is characteristic of the dehydrated surface vanadium oxide species and its intensity increases with increasing surface vanadium oxide coverage (Figs. 5 and 6) [38,43]. At low surface vanadium oxide coverage (1% V_2O_5), the surface silanol groups exhibit with a Raman band at 968 cm^{-1} which disappears during methanol oxidation due to the formation of surface methoxy groups on SiO_2. The absence of the 968 cm^{-1} Raman band for the dehydrated 7% V_2O_5/SiO_2 sample prior to reaction indicates that the surface silanol groups are primarily titrated by the surface vanadium oxide species. The Raman features of the surface vanadium

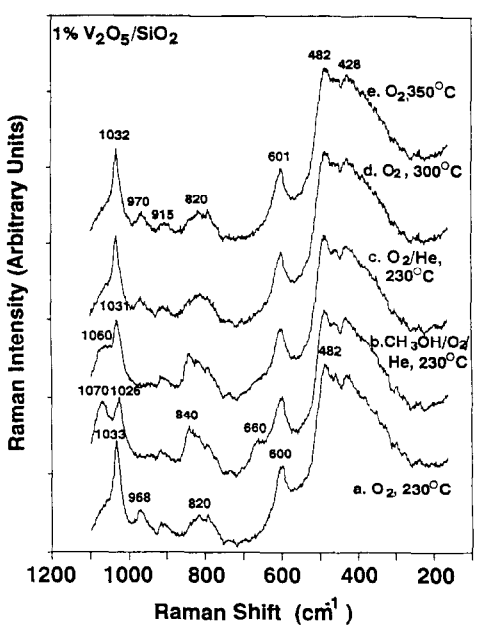

Fig. 5. In situ Raman spectra of the 1% V_2O_5/SiO_2 catalyst at various stages of methanol oxidation reaction in the 100–1200 cm^{-1} region.

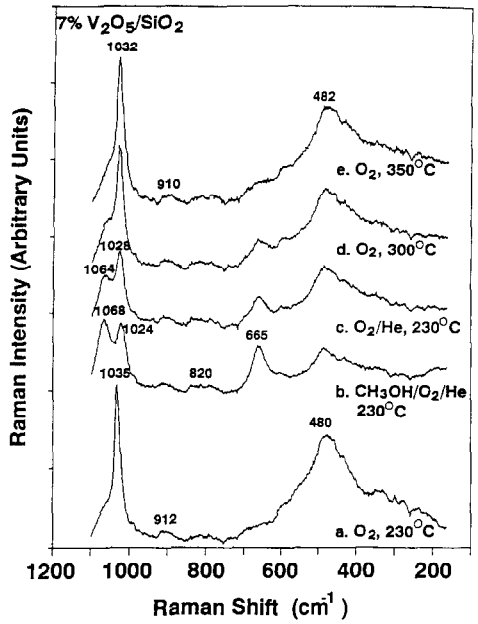

Fig. 6. In situ Raman spectra of the 7% V_2O_5/SiO_2 catalyst at various stages of methanol oxidation reaction in the 100–1200 cm^{-1} region.

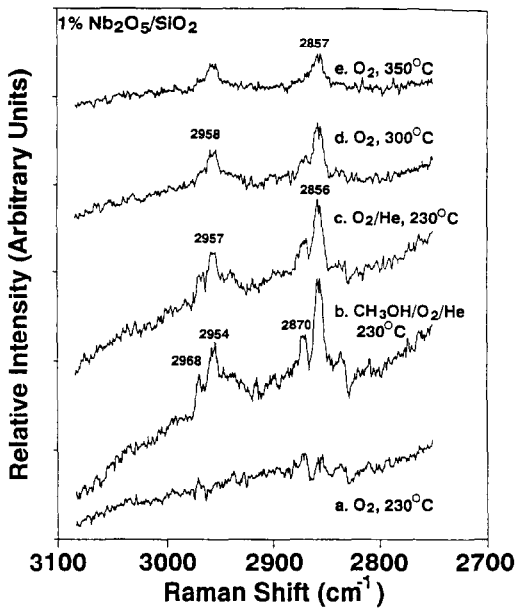

Fig. 7. In situ Raman spectra of the 1% Nb_2O_5/SiO_2 catalyst at various stages of methanol oxidation reaction in the 2700–3100 cm^{-1} region.

oxide species are altered in the presence of adsorbed methanol molecules. The Raman intensity of the dehydrated surface vanadium oxide species (1033-1035 cm^{-1}) decreases and the band shifts 5-10 cm^{-1} toward lower wavenumber and additional Raman bands appear at ~ 1070 and ~ 665 cm^{-1}. Raman bands at ~ 1070 and ~ 665 cm^{-1} are associated with V-alkoxide compounds and have been assigned to terminal V = O and bridging V-O-R vibrations, respectively [44]. The initial dehydrated Raman features are obtained after reoxidation of the catalyst at 350°C under flowing oxygen. Crystalline V_2O_5 Raman features (~ 994, ~ 702, ~ 527, ~ 404, ~ 284 and ~ 146 cm^{-1}) were not observed in this series of experiments.

3.1.3. Nb_2O_5/SiO_2

The in situ Raman spectra of the 1% Nb_2O_5 and 5% Nb_2O_5/SiO_2 catalysts during methanol oxidation are shown in Figs. 7–10. Raman features of the surface methoxy groups appear at 2954 and 2856 cm^{-1} for the low surface niobium oxide coverage and only very weak surface methoxy Raman features are present for the higher surface niobium oxide coverage indicating that most of the surface hydroxyl groups of

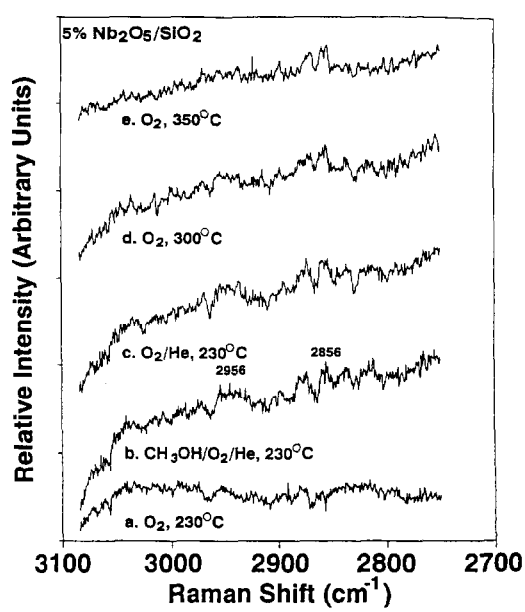

Fig. 8. In situ Raman spectra of the 5% Nb_2O_5/SiO_2 catalyst at various stages of methanol oxidation reaction in the 2700–3100 cm^{-1} region.

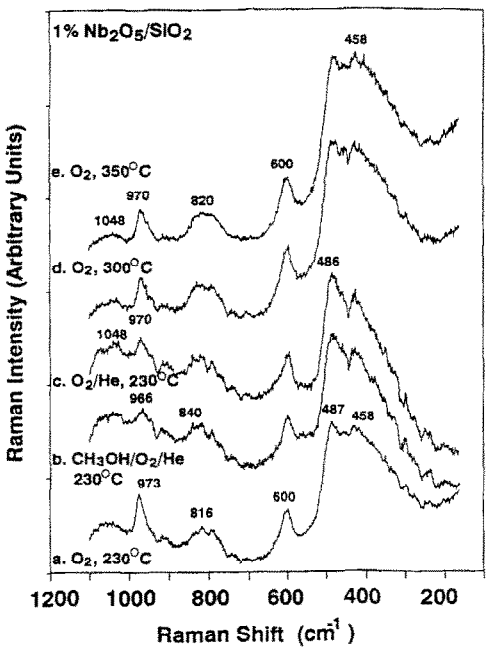

Fig. 9. In situ Raman spectra of the 1% Nb_2O_5/SiO_2 catalyst at various stages of methanol oxidation reaction in the 100–1200 cm^{-1} region.

the silica support have been titrated by the surface niobium oxide species (see Figs. 7 and 8). For the 1% Nb_2O_5/SiO_2 sample, the Raman band of the surface niobium oxide species possesses a Raman band at ~ 973 cm^{-1} [29] which overlaps with the surface silanol groups (Raman band at ~ 970 cm^{-1}). The Raman intensity of the dehydrated surface niobium oxide species decreases in the presence of methanol oxidation environment (see Figs. 9 and 10) and cannot be totally restored to its original intensity upon reoxidation of the Nb_2O_5/SiO_2 catalysts at 350°C. Crystalline Nb_2O_5 Raman features (~ 680 and ~ 250 cm^{-1}) were not observed in this series of experiments.

3.1.4. CrO_3/SiO_2

The dehydrated silica-supported chromium oxide catalysts possess a Raman band at ~ 986 cm^{-1} which is characteristic of the dehydrated surface chromium oxide species [19]. Previous Raman and DRS studies on the CrO_3/SiO_2

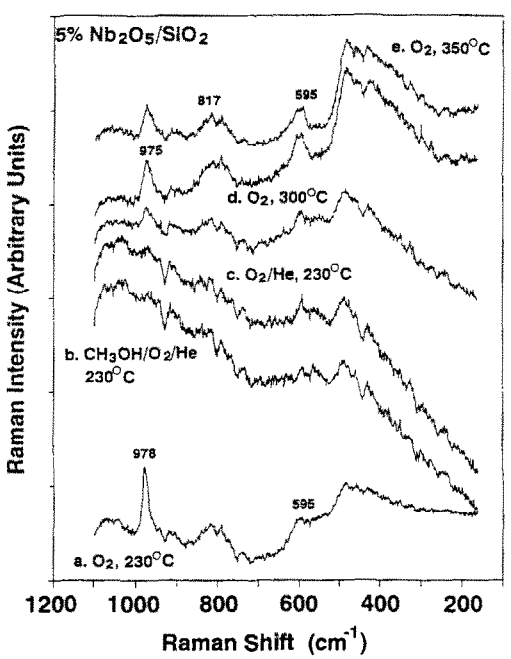

Fig. 10. In situ Raman spectra of the 5% Nb_2O_5/SiO_2 catalyst at various stages of methanol oxidation reaction in the 100–1200 cm^{-1} region.

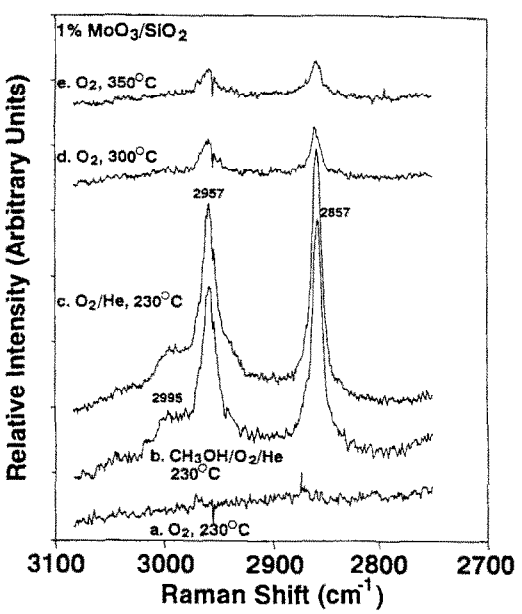

Fig. 11. In situ Raman spectra of the 1% MoO_3/SiO_2 catalyst at various stages of methanol oxidation reaction in the 2700–3100 cm^{-1} region.

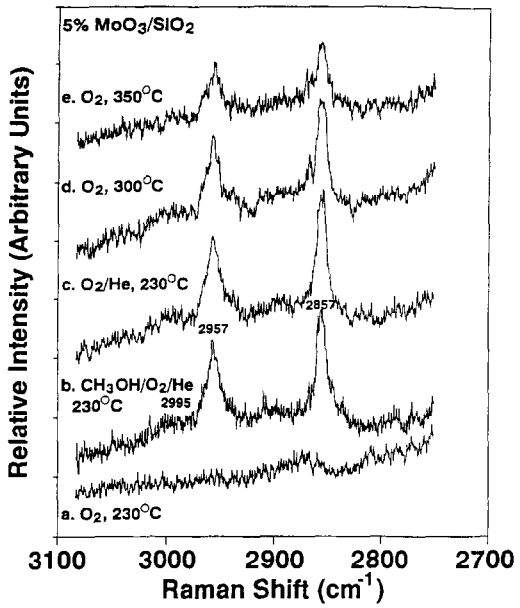

Fig. 12. In situ Raman spectra of the 5% MoO_3/SiO_2 catalyst at various stages of methanol oxidation reaction in the 2700–3100 cm^{-1} region.

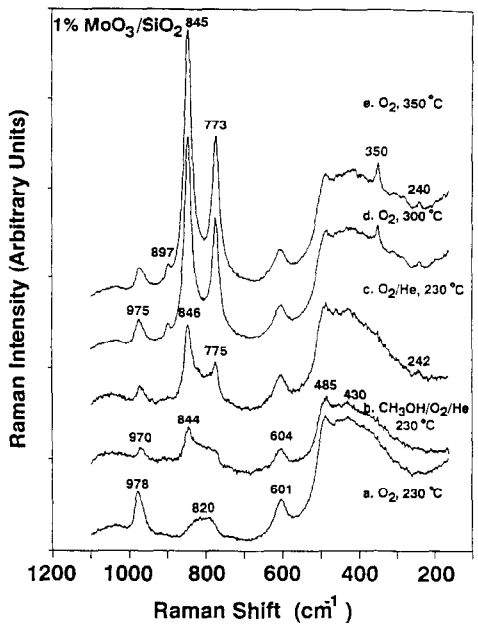

Fig. 13. In situ Raman spectra of the 1% MoO_3/SiO_2 catalyst at various stages of methanol oxidation reaction in the 100–1200 cm^{-1} region.

systems indicate that the dehydrated surface chromium oxide species with a tetrahedral CrO_4 structure is predominantly present on the silica surface [17,18]. However, a fluorescence background is induced and overshadows the Raman features of the surface chromium oxide species under methanol oxidation reaction.

3.1.5. MoO_3/SiO_2

The in situ Raman spectra of 1% MoO_3 and 5% MoO_3/SiO_2 catalysts during methanol oxidation are shown in Figs. 11–14. The adsorbed surface methoxy groups on these two samples are very similar to that on the silica support and exhibit Raman band at 2995, 2957 and 2857 cm^{-1} (see Figs. 11 and 12). The decrease of the Raman intensities of the surface methoxy species of the higher surface molybdenum oxide coverage indicating that most of the surface hydroxyl groups of the silica support have been titrated by the surface molybdenum oxide species (see Figs. 11 and 12). Molybdenum oxide forms a surface molybdenum oxide overlayer on the silica support due to the absence of Raman

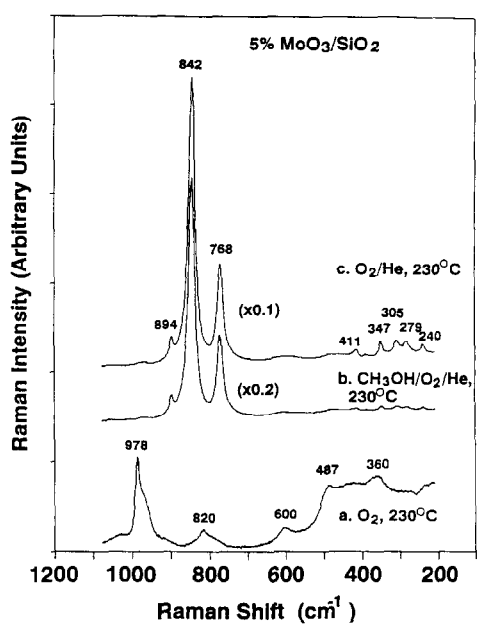

Fig. 14. In situ Raman spectra of the 5% MoO_3/SiO_2 catalyst at various stages of methanol oxidation reaction in the 100–1200 cm^{-1} region.

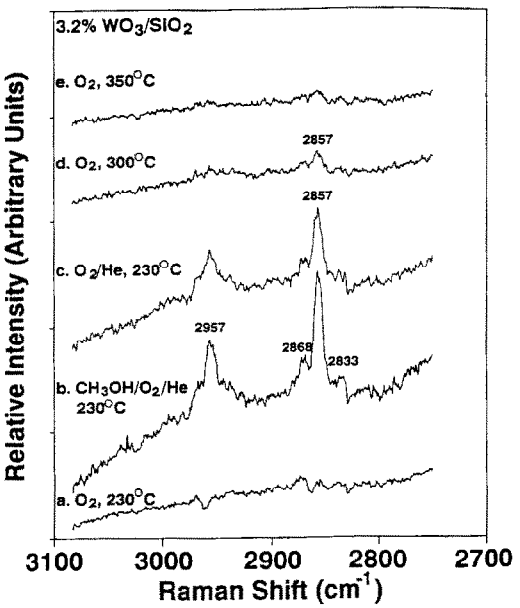

Fig. 15. In situ Raman spectra of the 3.2% WO_3/SiO_2 catalyst at various stages of methanol oxidation reaction in the 2700–3100 cm^{-1} region.

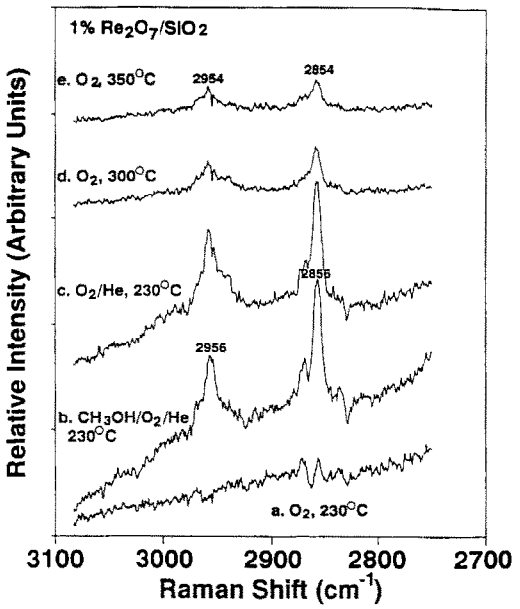

Fig. 17. In situ Raman spectra of the 1% Re_2O_7/SiO_2 catalyst at various stages of methanol oxidation reaction in the 2700–3100 cm^{-1} region.

features of crystalline α-MoO_3 (major Raman bands at 994, 816 and 284 cm^{-1}). The dehydrated surface molybdenum oxide species (Raman band at 978 cm^{-1}) are transformed into microcrystalline β-MoO_3 particles with weak Raman bands at 844 and 775 cm^{-1} [27]. The

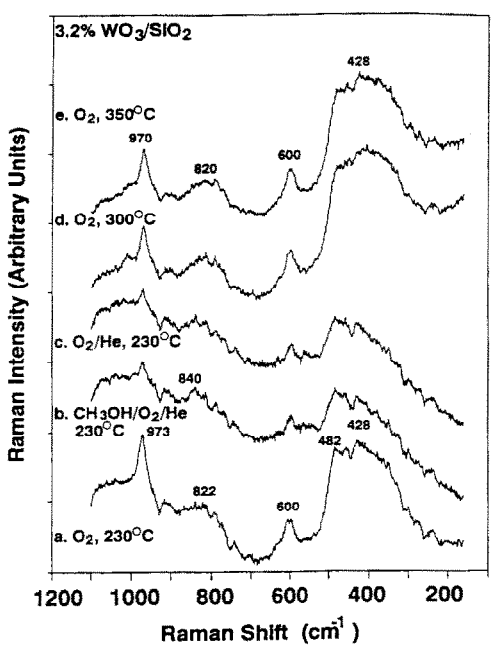

Fig. 16. In situ Raman spectra of the 3.2% WO_3/SiO_2 catalyst at various stages of methanol oxidation reaction in the 100–1200 cm^{-1} region.

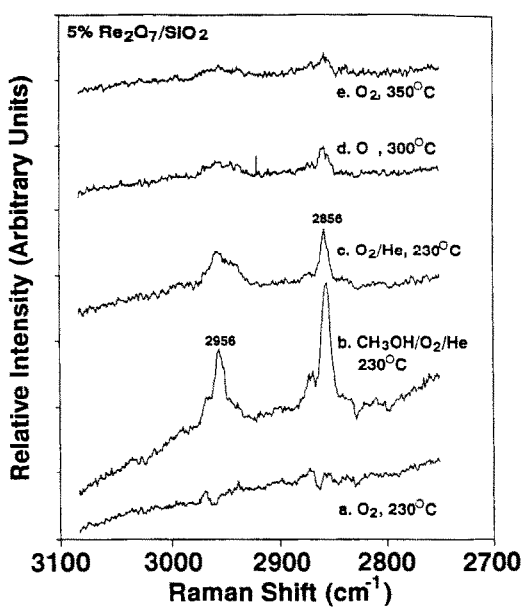

Fig. 18. In situ Raman spectra of the 5% Re_2O_7/SiO_2 catalyst at various stages of methanol oxidation reaction in the 2700–3100 cm^{-1} region.

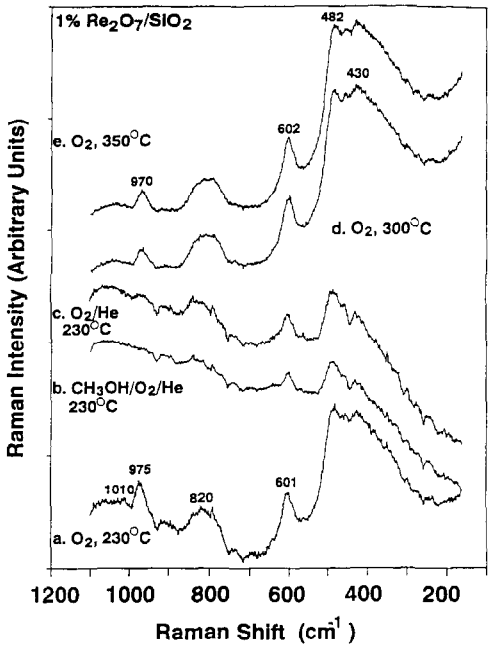

Fig. 19. In situ Raman spectra of the 1% Re_2O_7/SiO_2 catalyst at various stages of methanol oxidation reaction in the 100–1200 cm^{-1} region.

microcrystalline β-MoO_3 particles transform into a larger crystalline particles with strong Raman bands at ~897, ~845, ~770 and ~350 cm^{-1} at higher molybdenum oxide coverage and higher calcination temperatures (see Figs. 13 and 14).

3.1.6. WO_3/SiO_2

The in situ Raman spectra of the silica-supported tungsten oxide catalyst during methanol oxidation are shown in Figs. 15 and 16. The surface methoxy groups contain Raman bands at 2957 and 2857 cm^{-1} (see Fig. 15). The Raman band at 973 cm^{-1} in Fig. 16 is characteristic of the dehydrated surface tungsten oxide species [41]. The Raman intensity of the dehydrated surface tungsten oxide species decreases in the presence of the methanol oxidation reaction environment and a fluorescence background is induced. The surface tungsten oxide species can not be totally restored upon the reoxidation of the sample at a temperature of 350°C (see Fig. 16). Crystalline WO_3 Raman features (~805, ~710 and ~320 cm^{-1}) were not observed in this series of experiments.

3.1.7. Re_2O_7/SiO_2

The in situ Raman spectra of the 1% Re_2O_7/SiO_2 and 5% Re_2O_7/SiO_2 samples under reaction conditions are shown in Figs. 17–20. The surface methoxy groups with Raman bands at 2956 and 2856 cm^{-1} form on the catalyst surface and the Raman intensities of the surface methoxy groups decrease with the higher temperature oxidation treatments (see Figs. 17 and 18). The Raman bands at 1010, 973 and 340 cm^{-1} are characteristic of the dehydrated surface rhenium oxide species [31]. Under reaction conditions, the surface rhenium oxide species become volatile which is reflected in the absence of the Raman features of the surface rhenium oxide species after reoxidation of the samples at higher temperatures.

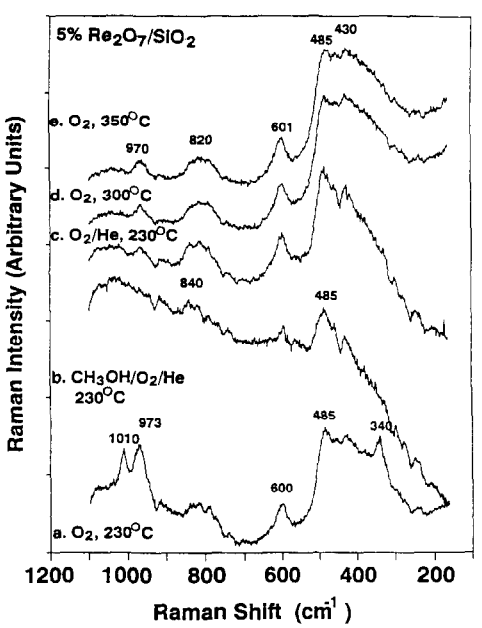

Fig. 20. In situ Raman spectra of the 5% Re_2O_7/SiO_2 catalyst at various stages of methanol oxidation reaction in the 100–1200 cm^{-1} region.

4. Discussion

The in situ Raman experiments during methanol oxidation reveal that surface methoxy species were formed on the silica surface as well as the surface methoxy data are summarized in Table 1. The surface $Si\text{-}OCH_3$ species (Raman bands at 2856, 2958 and 2990 cm^{-1}) by adsorbed methanol as shown in Figs. 1 and 2. The number of available surface Si-OH sites for methanol adsorption generally decreased with increasing metal oxide loading because of the surface metal oxide species also titrated the surface Si-OH sites (compare the dehydrated spectra in Fig. 2, Figs. 5 and 6). For the V_2O_5/SiO_2 system, additional strong surface methoxy Raman vibrations at 2932 and 2830 cm^{-1} were also present and have been assigned to the formation of surface $V\text{-}OCH_3$ species because of the simultaneous appearance of V = O and V-O-R Raman bands at 1070 and 665 cm^{-1} (see Figs. 5 and 6). For the other silica supported metal oxide systems, the surface methoxy groups are essentially located on the silica support. Oyama has previously proposed that the surface vanadia species is somewhat basic towards alcohols, which are mildly acidic and that this is the reason for the preferential coordination of the surface alkoxy species to the surface vanadia species rather than the somewhat acidic surface Si-OH site [45,46]. Along those lines of thinking, the preferential coordination of the surface methoxy species to the silica support for the supported niobium oxide and tungsten oxide systems suggests that these oxides are more acidic than vanadia and agrees with the known acidic character of these metal oxides. The stability of the above surface methoxy species after the methanol oxidation reaction in an O_2/He stream suggests that these are primarily 'spectator' surface methoxy species that do not participate in the methanol oxidation reaction. Nevertheless, their behavior does provide some insight into the preferential interactions of methanol with the different surface sites present in the silica supported metal oxide catalysts.

The dynamic nature of the silica supported surface metal oxide species during methanol oxidation was revealed by in situ Raman spectroscopy studies. The surface metal oxide species were found to form stable surface $M\text{-}OCH_3$ complexes, volatile $M\text{-}OCH_3$ complexes, crystalline metal oxide particles or partially reduced surface metal oxide species during methanol oxidation. The Raman bands for the surface metal oxide species before and during methanol oxidation are summarized in Table 2. As mentioned above, extensive formation of stable surface $M\text{-}OCH_3$ species was only found for the V_2O_5/SiO_2 system (Raman bands at 1070 and 660 cm^{-1}). The mobility of the surface rhenium

Table 1
Raman frequencies of the surface methoxy species on the silica-supported metal oxide catalysts

	$Si\text{-}OCH_3$ (asym. C–H)	$Si\text{-}OCH_3$ (sym. C–H)	$M\text{-}OCH_3$	$Si\text{-}OCH_3$ (sym. C–H)	$M\text{-}OCH_3$
SiO_2	2990(w)	2958(s)		2856(s)	
1% V_2O_5/SiO_2	2990(w)	2957(s)	2931(m)	2857(s)	2834(m)
7% V_2O_5/SiO_2		2954(m)	2930(s)	2854(m)	2832(m)
1%Nb_2O_5/SiO_2		2954(s)		2856(s)	
5% Nb_2O_5/SiO_2		2956(vw)		2856(vw)	
1% CrO_3/SiO_2		[a]		[a]	
1% MoO_3/SiO_2	2995(w)	2957(s)		2857(s)	
5% MoO_3/SiO_2	2995(w)	2957(s)		2857(s)	
3.2%WO_3/SiO_2		2957(s)		2857(s)	
1% Re/SiO_2		2956(s)		2856(s)	
5% Re/SiO_2		2956(s)		2856(s)	

[a] Fluorescence under reaction conditions.

Table 2
Raman frequencies of the surface metal oxide species before and during methanol oxidation reaction

	Before reaction			During reaction					
1% V_2O_5/SiO_2	1033			1070	1026			660	
7% V_2O_5/SiO_2	1035			1068	1024			665	
1%Nb_2O_5/SiO_2		973				966			
5% Nb_2O_5/SiO_2		978				[a]			
1% CrO_3/SiO_2		986				[a]			
1% MoO_3/SiO_2		978				970		844	775
5% MoO_3/SiO_2		978	360				894	842	768
3.2%WO_3/SiO_2		973				973			
1% Re/SiO_2	1010	975				[b]			
5% Re/SiO_2	1010	975	340			[b]			

[a] Fluorescence under reaction conditions.
[b] Absent due to volatilization.

oxide and molybdenum oxide species on the silica support is attributed to the formation of M-OCH_3 complexes and these interactions resulted in the volatilization of the surface rhenium oxide species and the crystallization of the surface molybdenum oxide species. The Mo-OCH_3 species were also somewhat volatile because Mo deposits were detected on the glass portion of the reactor exit [27]. The volatility of Mo and Re oxides are well known, but are enhanced by the formation of the M-OCH_3 complexes. The Raman bands for the terminal M = O bonds generally decreased in intensity and shifted to lower wavenumbers during methanol oxidation (see Table 2). These changes reflect the net reducing environment of the methanol oxidation reaction and the presence of adsorbed methoxy species on the catalyst surface, respectively. The shift to lower wavenumbers may be due to hydrogen bonding of the terminal M = O bonds with the surface methoxy species. The reduced surface metal oxide species did not give rise to new Raman bands and additional information about the reduced species should be obtainable from DRS and EPR spectroscopies [18]. The inability to completely reoxidize the surface niobium oxide and tungsten oxide species after methanol oxidation may be related to the residual amounts of adsorbed surface methoxy on the catalyst surface even after high temperature oxidation. Thus, the behavior of the silica supported metal oxide species during methanol oxidation depends on the intrinsic properties of the surface metal oxide.

Table 3
Catalytic properties of methanol oxidation reaction over the supported metal oxide on silica (Cab-O-Sil, HS-5) catalysts

	Activity	TOF	Selectivity				
	(mol CH_3OH/g h)	(s^{-1})	FM	MF	DMM	CO_x	DME
SiO_2	2.6×10^{-4}					85	15
1% V_2O_5/SiO_2	3.9×10^{-4}	3.9×10^{-3}	72			17	17
1.5% V_2O_5/SiO_2	9.4×10^{-4}	1.6×10^{-3}	83			14	3
1% Nb_2O_5/SiO_2	2.7×10^{-2}	9.7×10^{-2}	32	52	3	6	7
2% Nb_2O_5/SiO_2	3.8×10^{-2}	7.0×10^{-2}	33	51	4	7	5
1% CrO_3/SiO_2	5.5×10^{-2}	1.4×10^{-1}	60	12	2	25	1
2% CrO_3/SiO_2	7.5×10^{-2}	1.1×10^{-1}	71	9	1	18	1
3% CrO_3/SiO_2	1.3×10^{-1}	1.1×10^{-1}	76	6	2	15	1
1% MoO_3/SiO_2	2.3×10^{-3}	9.0×10^{-3}	45	28	19	8	
1% WO_3/SiO_2	5.3×10^{-2}	3.4×10^{-1}	46	50		3	
1% Re_2O_7/SiO_2	2.4×10^{-3}	1.6×10^{-2}	10			89	1

The activity and selectivity properties of silica supported metal oxide catalysts for methanol oxidation have been reported in the literature and are summarized in Table 3. The silica employed in these studies was Cab-O-Sil (HS-5) which has a slightly lower surface hydroxyl density than the silica employed in the present in situ Raman studies. Comparative methanol oxidation catalytic studies demonstrated that similar results were obtained for surface vanadia species on both silica supports [47]. The silica support gave rise to CO_x and dimethyl ether products and did not yield any redox products (formaldehyde, methyl formate and dimethoxymethane). The CO_x was produced from the oxidation of the Si-OCH_3 species which is a very slow reaction as reflected by the low catalyst activity and the stability of the Si-OCH_3 species in the in situ Raman studies. The dimethyl ether is produced by some acidic impurities present in the catalyst. The addition of surface metal oxide species to the silica support resulted in the production of redox products (formaldehyde, methyl formate and dimethoxymethane). The silica supported surface rhenium oxide produced small amounts of formaldehyde. The low selectivity towards redox products reflects the low surface concentration of surface rhenium oxide species due to its volatilization. In contrast, the silica supported surface vanadia species yielded a high selectivity towards redox products and especially formaldehyde. The uniquely high formaldehyde selectivity and absence of methyl formate production for the V_2O_5/SiO_2 catalyst may be related to the preferential formation of surface V-OCH_3 species during methanol oxidation. The other supported metal oxide catalysts yielded high selectivities towards formaldehyde as well as methyl formate. Methyl formate production requires the reaction between formaldehyde produced on a redox site and adjacent surface methoxy species on the silica support. The in situ Raman studies revealed that these supported metal oxide catalytic systems possess significant surface concentrations of Si-OCH_3. Indeed, the production of methyl formate for the silica supported chromium oxide system tracks the available surface hydroxyls concentration (decreases with coverage and high calcination temperatures that remove the surface hydroxyls) [19,27]. Thus, the in situ Raman measurements during methanol oxidation provide a fundamental basis for the selectivity differences among the series of silica supported metal oxide catalysts.

A surprising result is that oxides that are generally considered acidic and somewhat nonreducible, tungsten oxide and niobium oxide, exhibit a high selectivity to redox products when supported on silica. Similarly, surface titania on silica also gives rise to a high selectivity of redox products during methanol oxidation [42], but bulk TiO_2 yields almost no redox products [48]. In contrast, no redox products are produced during methanol oxidation when surface tungsten oxide and niobium oxide are present on a reducible oxide support such as titania [48] or a nonreducible oxide support such as alumina [29]. The mechanism by which silica ligands induce redox properties in such typically acidic oxides is currently not understood.

The catalytic activities of the supported metal oxide catalysts for methanol oxidation were generally significantly greater than the pure silica support, which demonstrated that the observed catalytic properties are associated with the surface metal oxide species (see Table 3). The V_2O_5/SiO_2 catalytic system was only slightly more active among than the pure silica support and the least active among the silica supported metal oxide catalytic systems. This low catalytic activity may be related to the stability of the surface V-OCH_3 complexes formed during methanol oxidation. The Re_2O_7/SiO_2 catalytic system was approximately an order of magnitude more active than the pure silica support which indicates that not all the surface rhenium oxide species volatilized during methanol oxidation and some residual rhenium oxide was still present on the support (also reflected in the small amounts of formaldehyde produced for this catalyst). The other

silica-supported metal oxide catalysts were approximately two orders of magnitude more active than the pure silica support for the oxidation of methanol. The apparent turnover frequencies of the different silica-supported metal oxide catalysts during methanol oxidation are also shown in Table 3: W > Cr > Nb > Mo ~ Re ≫ V. The TOF values are only apparent for the supported Mo and Re systems due to the partial crystallization and volatilization of these surface oxides during methanol oxidation and, consequently, the intrinsic TOF values for these two oxides are actually somewhat higher (especially the supported rhenium oxide catalyst where extensive volatilization has occurred).

Comparison of the methanol oxidation TOF values for the silica-supported metal oxides with corresponding methanol oxidation studies of these oxides on the reducible titania support is very informative [49]. The TOF values for these titania-supported metal oxides were found to be V ($1\text{-}3 \times 10^{0}$ s^{-1}) ~ Re (1×10^{0} s^{-1}) ≫ Mo ($2\text{-}6 \times 10^{-1}$ s^{-1}) ~ Cr ($1\text{-}3 \times 10^{-1}$ s^{-1}) ⋙ W (1×10^{-2} s^{-1}) ~ Nb (8×10^{-3} s^{-1}). The activities of the titania-supported tungsten oxide and niobium oxide catalysts were only slightly above that for the pure titania support and no redox products were formed. For the titania-supported metal oxide catalyst, volatilization or crystallization of the surface metal oxides did not occur during methanol oxidation [50]. The methanol oxidation TOF values for the titania-supported metal oxide catalysts almost follow an inverse trend when compared to the silica-supported metal oxide catalysts. The catalytic activities of the titania–supported metal oxide catalysts are more typical of the methanol oxidation activity observed with other oxide supports [49]. The mechanism by which silica ligands activates the redox properties of surface metal oxide species, especially nonreducible surface oxides such as niobium oxide and tungsten oxide, is currently not understood.

The redox properties of metal oxide-silica systems has received much attention in recent years because of the commercial success of the Ti-silicalite molecular sieve catalyst [51]. In recent years studies have focused on the incorporation of V into the silicalite structure [52–54]. Comparison of the catalytic properties of amorphous silica-supported titania and vanadia catalysts with the corresponding silicalite catalyst systems for vapor phase methanol oxidation has given almost identical TOF values and redox selectivities for the corresponding systems [55,56]. These results suggest that the vapor phase catalytic oxidation activity of the metal oxides are controlled by the silica ligands rather than the extent of crystallinity of the silica matrix. The current studies further suggest that successful incorporation of oxides of W, Nb and Cr into the silicalite matrix would result in much more active and selective catalysts than Ti-silicalite and V-silicalite. Unfortunately, this is not an easy task or may even not be possible [57].

5. Conclusions

The in situ Raman spectra of silica-supported metal oxide catalysts (surface oxides of V, Nb, Cr, Mo, W and Re) were measured during methanol oxidation. The methanol adsorbed as surface methoxy species on the surface Si-OH groups and only formed stable surface M-OCH_3 complexes for the V_2O_5/SiO_2 system. All the surface metal oxide species on silica were modified by the methanol oxidation environment. Surface rhenium oxide species were volatilized and surface molybdenum oxide species were partially transformed to crystalline β-MoO_3 particles via the formation of Re-methoxy and Mo-methoxy complexes, respectively. the surface niobium oxide and tungsten oxide species were partially reduced by the net reducing methanol oxidation environment. In situ Raman spectra for the CrO_3/SiO_2 catalysts could not be obtained due to sample fluorescence of the reduced chromium oxide species. Comparison of the methanol oxidation redox selectivity and activity with the in situ Raman spectra provided

a fundamental basis for the observed catalytic trends. Formaldehyde was exclusively formed with surface vanadia species due to the preferential formation of V-OCH_3 complexes. The other surface metal oxide species generally yielded both formaldehyde and methyl formate with the latter product originating from the surface methoxy species on the silica surface. The catalytic activities of the silica-supported metal oxide catalysts were generally much higher than that of the pure silica support and the TOF values followed the pattern: W > Cr > Nb > Mo ~ Re > V. The mechanism by which the silica support ligands activate these surface metal oxide species for redox catalytic reactions is not completely understood since their reactivity pattern is very different than found when other oxide supports are employed for these surface metal oxide species.

Acknowledgements

The financial support of the National Science Foundation (grant no. CTS-9417981) is gratefully acknowledged.

References

[1] J.P. Hogan and R.L. Barks, Belg. Pat., 53067, 1955.
[2] J.P. Hogan, D.D. Norwood and C.A. Ayres, J. Appl. Polym. Sci., 36 (1981) 49.
[3] C.L. Thomas, Catalytic Processes and Proven Catalysis, Academic Press, New York, 1970.
[4] S.T. Oyama and G.A. Somorjai, J. Phys. Chem., 94 (1990) 5022.
[5] S.T. Oyama, A.M. Middlebrook and G.A. Somorjai, J. Phys. Chem., 94 (1990) 5029.
[6] A. Erdohelyi an F. Solymosi, J. Catal., 123 (1990) 31.
[7] L. Owens and H.H. Kung, J. Catal., 144 (1993) 202.
[8] J. Le Bars, J.C. Vedrine, A. Auroux, S. Trantmann and M. Baerns, Appl. Catal. A, 88 (1992) 179.
[9] M. de Boer, A.J. van Dillen, D.C. Koningsberger, J.W. Geus, M.A. Vuurman and I.E. Wachs, Catal. Lett., 11 (1991) 227.
[10] N.D. Spencer, C.J. Pereira and R.K. Grasselli, J. Catal., 126 (1990) 546.
[11] M.A. Banares, J.L.G. Fierro and J.B. Moffat, J. Catal., 142 (1993) 406.
[12] J.C. Mol and J.A. Moulijn, in J.R. Anderson and M. Boudart (Editors), Catalysis: Science and Technology, Springer-Verlag, Berlin, Heidelberg, 1987, p. 69.
[13] R. Merryfield, M.P. McDaniel and G. Parks, J. Catal., 77 (1982) 348.
[14] M.P. McDaniel and M.M. Johnson, J. Catal., 101 (1986) 446.
[15] A. Ellison, J. Chem. Soc., Faraday Trans. 1, 80 (1984) 2567.
[16] D.D. Beck and J.H. Lunsford, J. Catal., 68 (1981) 121.
[17] J.-M. Jehng, I.E. Wachs, B.M. Weckhuysen and R.A. Schoonheydt, J. Chem. Soc., Faraday Trans., 91 (1995) 953.
[18] B.M. Weckhuysen, R.A. Schoonheydt and I.E. Wachs, Chem. Rev., in press.
[19] D.S. Kim, J.M. Tatibouet, I.E. Wachs, J. Catal., 136 (1992) 209.
[20] S.T. Oyama, G.T. Went, K.B. Lewis, A.T. Bell and G.A. Somorjai, J. Phys. Chem., 93 (1989) 6786.
[21] S.T. Oyama, J. Catal., 128 (1991) 210.
[22] G. Deo, I.E. Wachs and J. Haber, Crit. Rev. Surf. Chem., 40 (1994) 1.
[23] T. Ono, M. Anpo and Y. Kubokawa, J. Phys. Chem., 90 (1986) 4780.
[24] T.C. Liu, M. Forissier, G. Coudurier and J.C. Vedrine, J. Chem. Soc., Faraday Trans. 1, 85 (1989) 1807.
[25] M. Che, C. Louis and J.M. TatiBouet, Polyhedron, 5 (1986) 123.
[26] Y. Barbaux, A.R. Elamrani, E. Payen, L. Genzenbre, J.P. Bonnelle and B. Grzybowska, Appl. Catal., 44 (1988) 117.
[27] M.A. Banares, H. Hu and I.E. Wachs, J. Catal., 150 (1994) 407.
[28] M.A. Banares, H. Hu and I.E. Wachs, J. Catal., (1995).
[29] J.-M. Jehng and I.E. Wachs, Catal. Today, 16 (1993) 417.
[30] H. Hu, I.E. Wachs and S.R. Bare, J. Phys. Chem., 99 (1995) 10897.
[31] M.A. Vuurman, D.J. Stufkens, A. Oskam and I.E. Wachs, J. Mol. Catal., 76 (1992) 263.
[32] M.A. Vuurman, I.E. Wachs, D.J. Stufkens and A. Oskam, J. Mol. Catal., 80 (1993) 209.
[33] G. Deo and I.E. Wachs, J. Catal., 129 (1991) 307.
[34] J.-M. Jehng and I.E. Wachs, J. Phys. Chem., 95 (1991) 7373.
[35] D.S. Kim and I.E. Wachs, J. Catal., 142 (1993) 166; M. Cornac, A. Janin and J.C. Lavalley, Polyhedron, 5 (1986) 183.
[36] M. Mauge, J.P. Gallas, J.C. Lavalley, G. Busca, G. Ramis and V. Lorenzelli, Hikrochim. Acta, II (1988) 57.
[37] N. Das, H. Eckert, H. Hu, I.E. Wachs, J. Walzer and F. Feher, J. Phys. Chem., 97 (1993) 8240.
[38] S. Yoshida, T. Tanaka, T. Hanada, T. Hiraiwa and H. Kanai, Catal. Lett., 12 (1992) 277.
[39] B.A. Morrow, C.W. Thomson and R.W. Wetmore, J. Catal., 28 (1973) 332.
[40] B.M. Weckhuysen, F. Pelgrims, H. Leeman, R.A. Schoonheydt, G. Deo, J.-M. Jehng, H. Hu and I.E. Wachs, submitted.
[41] D.S. Kim, M. Ostromecki, I.E. Wachs, S.D. Kohler and J.G. Ekerdt, Catal. Lett., (1995).
[42] J.M. Jehng and I.E. Wachs, Catal. Lett., 13 (1992)9.
[43] H. Eckert and I.E. Wachs, J. Phys. Chem., 93 (1989) 6796.
[44] F.D. Hardcastle and I.E. Wachs, J. Phys. Chem., 95 (1991) 5031.

[45] S.T. Oyama and G.A. Somorjai, Symp. Oxygen Activation, 199th ACS Natl. Meeting, Boston, MA, 22-27 April 1990, Prepr. Petrol. Chem. Div., ACS.
[46] S.T. Oyama, Res. Chem. Interm., 15 (1991) 165.
[47] H. Hu, X. Gao and I.E. Wachs, submitted
[48] G. Deo and I.E. Wachs, J. Catal., 146 (1994) 335.
[49] I.E. Wachs, G. Deo, M.A. Vuurman, H. Hu, D.S. Kim and J.M. Jehng, J. Mol. Catal., 82 (1993) 443.
[50] H. Hu and I.E. Wachs, J. Phys. Chem., 99 (1995) 10922.
[51] Snamprogetti, US Pat., 4,410,501, (1983).
[52] M.S. Rigutto and van Bekkum, J. Mol. Catal., 81 (1993) 77.
[53] A.V. Kucherov and A.A. Slinkin, Zeolites, 7 (1987) 583.
[54] B.M. Weckhuysen, I.P. Vannijvel and R.A. Schoonheydt, Zeolites, 15 (1995) 482.
[55] G. Deo, A.M. Turek, I.E. Wachs, D.R.C. Huybrechts and P.A. Jacobs, Zeolites, 13 (1993) 365.
[56] M.S. Rigut to, H. van Bekkum, G. Deo and I.E. Wachs, submitted.
[57] B.M. Weckhuysen and R.A. Schoonheydt, Zeolites, 14 (1994) 360.